ISET Journal of Earthquake Technology, Paper No. 421, Vol. 39, No. 3, September 2002, pp. 121-138

SEISMIC RESPONSE REDUCTION OF STRUCTURES USING ELASTO-PLASTIC PASSIVE ENERGY DISSIPATION

K. Sathish Kumar*, K. Muthumani*, N. Gopalakrishnan*, B. Sivarama Sarma*, G.R. Reddy** and Y.M. Parulekar**

* Assistant Director, Structural Dynamics Laboratory
Structural Engineering Research Centre, Taramani, Chennai - 600 113

** Scientific Officer, Reactor Safety Division
Bhabha Atomic Research Centre, Trombay, Mumbai - 400 085

ABSTRACT

The strength-based design philosophy depending on the inherent ductility of structures is not suitable for lifeline structures like nuclear power plants where even non-structural damage is a severe safety problem. Design of supporting systems for pipelines carrying highly toxic or radioactive liquids is an important issue in the safety aspect for a nuclear power installation which is a key topic for researchers all around the world. Generally, these pipeline systems are designed to be held rigid by conventional snubber supports for protection from earthquakes. The piping design must balance seismic deformations and other deformations due to thermal effect. A rigid pipeline system using conventional snubber supports always leads to an increase in thermal stresses; hence, a rational seismic design for pipeline supporting systems becomes essential. Contrary to this rigid design, it is possible to design a flexible pipeline system and to decrease the seismic response by increasing the damping through the use of passive energy absorbing elements, which dissipate vibration energy. This paper presents the experimental and analytical studies carried out on yielding type elasto-plastic passive energy-absorbing (PEA) devices to be used as support devices for pipelines subjected to large seismic deformations.

KEYWORDS: Passive Energy Absorber, Passive Energy Dissipater, Yielding Device, Support Device, Pipeline

NOMENCLATURE

a - Height of triangular portion of the X-plate PEA element

b - Breadth of triangular portion of the X-plate PEA element

d - Displacement of the X-plate PEA element

d_y - Yield displacement of the X-plate PEA element

E - Elastic modulus of the X-plate PEA element

F_y - Yield force of the X-plate PEA element

H - Hardening rate of the X-plate PEA element

h - Damping ratio of the X-plate PEA element

K - Equivalent stiffness of the X-plate PEA element

n - Number of X-plate PEA elements

r - Ramberg-Osgood exponent

t - Thickness of the X-plate PEA element

y_0 - Elastic depth

α - Jennings constant

ΔE - Energy dissipated per cycle by the X-plate PEA element

σ_y - Yield strength of the X-plate PEA element

INTRODUCTION

Earthquakes are potentially devastating events which threaten lives, destroy property, and disrupt life-sustaining services and societal functions. Historically, seismic resistant design of structures has been based upon a combination of strength and ductility. For small, frequent earthquakes characterised by small deformations, the structure can be expected to remain in the elastic range, with all stresses well below yield levels. However, it is not reasonable to expect a traditional structure to respond elastically, when subjected to a major earthquake characterised by large deformations. Instead, the design engineer relies upon the inherent ductility of structure to prevent catastrophic failure, while accepting a certain level of structural and non-structural damage. However, this strength-based design philosophy is not suitable for lifeline structures like nuclear power plants where even non-structural damage is a severe safety problem. For example, the design of supporting system for pipelines carrying highly toxic or radioactive liquids is an important problem in the safety aspect for a nuclear power installation.

Presently, seismic design of pipeline systems in a nuclear plant is conducted under the rigid design philosophy, where large-sized rigid supports like snubbers are used as seismic supports. In the seismic support design, it is necessary to consider the thermal load in addition to the seismic load, and the snubbers are used as devices to resist seismic load and allow thermal movement of piping. As these devices are relatively expensive and complex mechanisms, more inexpensive and reliable devices (Kelly et al., 1972; Skinner et al., 1975) are desirable as alternative to snubbers.

Recently, many studies (Namita et al., 1991; Kokubo et al., 1995; Chiba and Kobayashi, 1992) have been performed to find more reliable and economical support concepts, and various kinds of high damping supports of elasto-plastic, visco-elastic, friction, and lead extrusion type, aiming to reduce seismic response, are being developed. An elasto-plastic device is basically a yielding type device that functions based on the energy dissipation achieved by way of deforming a metal plate of uniform thickness beyond its yield displacement in the post-elastic region. Hence, such a yielding device is not effective at low amplitudes below the yield displacement. However, this type of device is very effective at large displacement amplitudes and is cost-effective also. A visco-elastic device functions based on the energy dissipation achieved by the visco-elastic behaviour shown under shear loading by certain types of visco-elastic substances like natural rubber and neoprene. Such a visco-elastic device possesses re-centering capability and is effective even at very low displacement amplitudes. However, this device is not cost-effective, and its performance is severely affected due to temperature variation and due to chemical environment. A friction device is one which functions based on the frictional resistance created during two metal surfaces slipping over each other. Such a device is effective in providing energy dissipation to the system only after the occurrence of slip, and its performance is also quite unpredictable. However, this device is very effective for large force applications. A lead extrusion damper functions by way of extruding solid lead through a small orifice or by way of forcing a bulged shaft through a closed chamber containing solid lead. Such a lead extrusion device is effective only after the yielding of lead, and is highly suited for large force applications. Also, this device is not cost-effective.

In general, earthquake loading introduces large displacements in a structure, and under such large displacements, a yielding type elasto-plastic device made of X-shaped metal plates is expected to perform better. This device is also found to be cheaper and relatively easier to fabricate. Hence, such a device is chosen in the present study for identifying an alternative seismic support for pipeline systems against the conventional snubber support

To evaluate such an alternative seismic support for pipeline systems a cooperative study (Sathish Kumar et al., 2000; Gopalakrishnan et al., 2001; Sivarama Sarma et al., 2001) by SERC, Chennai and BARC, Mumbai was performed on yielding type elasto-plastic passive energy absorbing elements/device applied to piping systems. A X-shape metal yielding device was considered in the study, because it greatly increases the system damping, resulting in reduced seismic response. In the experimental study conducted, X-shape metal PEA elements having different plate thicknesses were subjected to tests of static, dynamic, fatigue and seismic type. The test results were correlated against analytical results obtained using a standard mathematical model. Again, these X-shape metal PEA elements were fitted to a simple pipe segment representing a single-degree-of-freedom (SDOF) system and subjected to shaking table tests, to study the reduction in the seismic response of the system. Similar shaking table tests were again conducted on a piping system made of three pipe segments, representing a three-dimensional (3D) system, attached with a yielding type elasto-plastic PEA device made of X-shape metal PEA elements, to study the seismic response reduction capability of such a device.

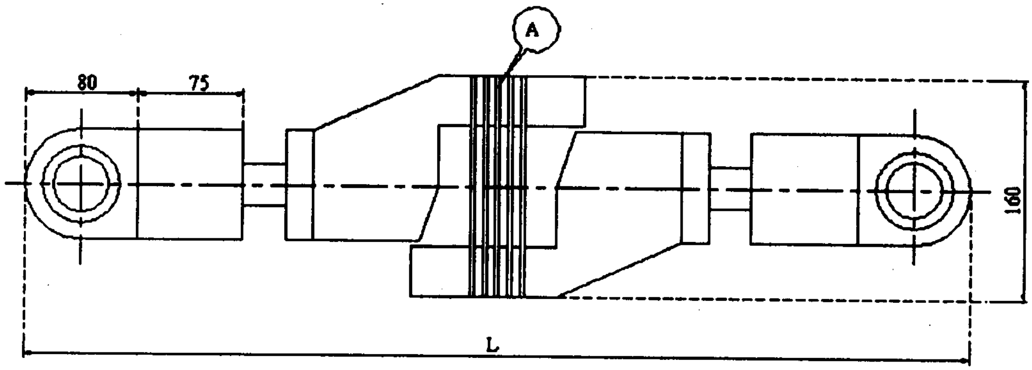

t	L
2	664
3	669
4	674
6	684

ALL DIMENSIONS ARE IN mm

(a) PEA device

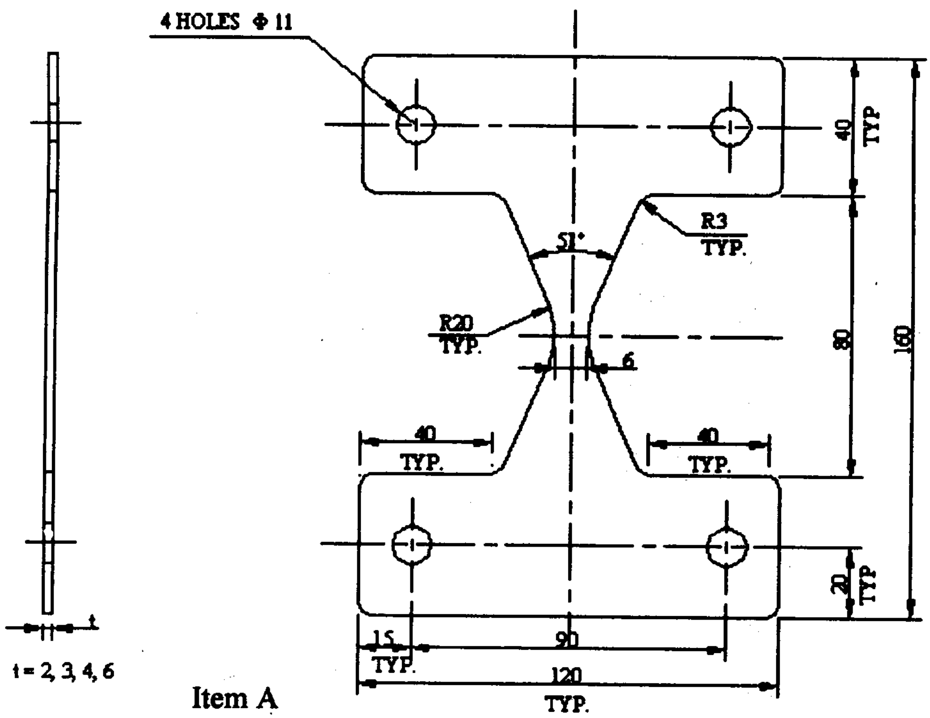

ALL DIMENSIONS ARE IN mm

(b) PEA element

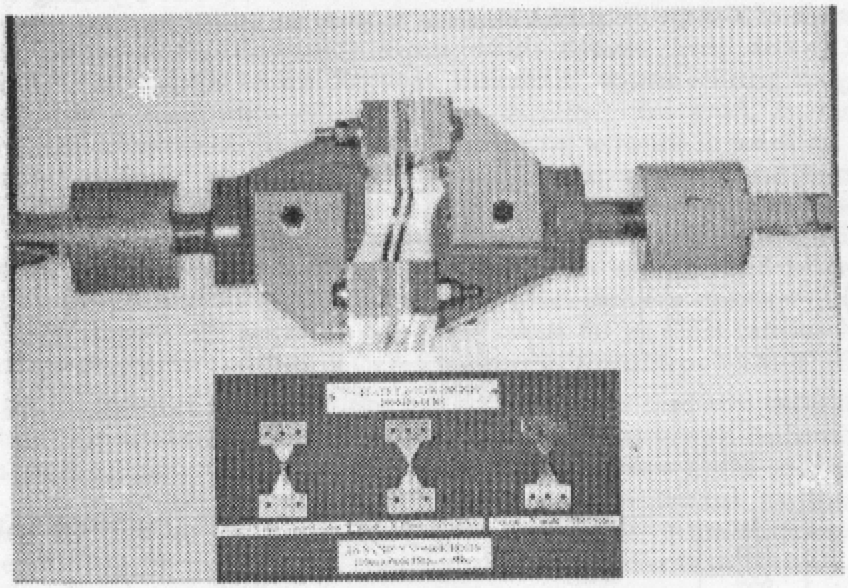

(c) Prototype of the yielding type elasto-plastic PEA device and X-plate PEA elements (inset) used inside the device

Fig. 1 Details of the yielding type elasto-plastic PEA device and X-plate PEA elements

Fig. 2 Test facility for the evaluation of PEA elements

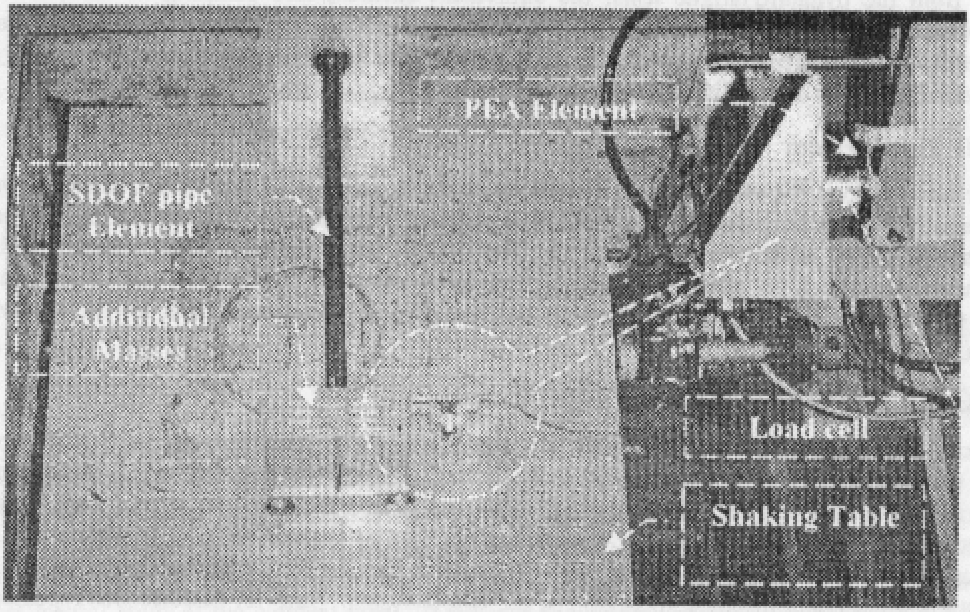

Fig. 3 SDOF pipe element attached with X-plate PEA element mounted on the shaking table, and close-up view

TESTING PROGRAM

1. PEA Elements / Device

The yielding type PEA element studied is basically made of a mild steel plate of uniform thickness having X shape in plan. The energy dissipation is achieved by deforming the X plate to plastic region. The force-displacement curve of such PEA element under dynamic loading shows non-linear hysteretic characteristics. From the energy dissipation of the hysteresis loop, the seismic response of the piping system is greatly reduced. Because mild steel is used in the plastic region, this region must be profiled to prevent plastic hinges from developing. To obtain this, a constant curvature has to be maintained along the length of the element, so that simultaneous yielding occurs at all sections. This was achieved by giving the mild steel plate an hourglass profile in plan resembling X shape, so that the breadth of the plate varies linearly along the length following the bending moment profile. When this X-shaped plate has large deformations, the plastic domain progresses in the thickness direction of the plate, leading to simultaneous yielding over the triangular region. Hence, a uniformly thick X-shape mild steel plate was chosen as a plate spring, in providing large energy dissipation to the system for reducing the seismic response. In the study conducted, the height and base of the triangle portion in an individual X-shaped plate element was kept as 40 mm and 40 mm, respectively. The overall height and width of the element was kept as 160 mm and 120 mm, respectively. Three different plate thickness values of 3, 4 and 6 mm were adopted for the PEA elements studied. The properties like yielding stress (σ_y), Elastic modulus (E) and Hardening rate (H) for the PEA element material were evaluated as 235 MPa, 1.94×10^5 MPa and 5.00×10^3 MPa, respectively. Figure 1 shows the details of the yielding type elasto-plastic PEA device, the individual PEA element used inside the device, and the prototype PEA device/element developed in the study.

2. Tests on the PEA Element

The PEA element was initially tested under static loading using the test facility created, as shown in Figure 2, by using a displacement-controlled actuator of 50 kN capacity. From the static force-displacement curves obtained, the elastic and inelastic behaviour of these PEA elements was studied. Then, using the same test facility, dynamic, fatigue and seismic loading tests were conducted on a similar element up to failure. For the dynamic and fatigue tests, sinusoidal loading of three different peak amplitudes of 5, 10 and 15 mm at 3.0 Hz was adopted. From the force-displacement (hysteretic) loops obtained from the dynamic/fatigue tests, the equivalent stiffness and damping of the individual PEA element were evaluated. For the seismic loading tests, a spectrum-compatible displacement time history for a specific site was generated and applied to the PEA element in succession up to failure. From the seismic test results, the design life of the PEA was evaluated.

3. SDOF Pipe Element

After having done the element level evaluation, the performance of these PEA elements was studied experimentally by attaching them to a simple pipe segment, representing a horizontal cantilever mounted on the shake table, as shown in Figure 3. The SDOF pipe element was provided with suitable arrangements for attaching additional masses and PEA elements at the free end. This is to achieve different fundamental frequencies, covering the maximum spectral response band for the chosen response spectrum.

4. Shaking Table Tests on the SDOF Pipe Element

Shaking table tests of sweep sine and seismic nature were conducted on the SDOF pipe element initially, without any PEA element attached to it. From the sweep sine test conducted, the system dynamic characteristics like stiffness and damping were evaluated. Similarly, from the seismic base excitation test conducted, the system seismic response was evaluated. Similar shaking table tests were again conducted on the same pipe element, attached with PEA elements of two different plate thickness values at the free end, to study the seismic response reduction of the whole system. Such an exercise was repeated for three more increased mass levels at the free end. From the seismic responses collected at the free end of SDOF pipe element before and after attaching the PEA elements to it, the seismic response reduction efficiency of different PEA elements was evaluated.

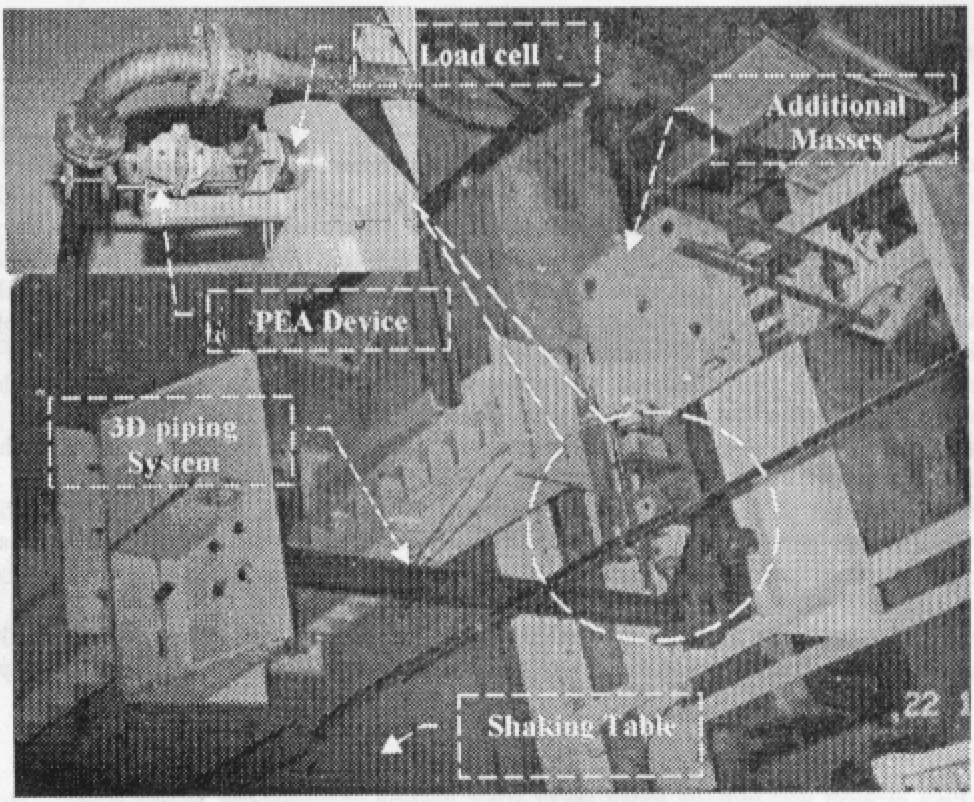

Fig. 4 3D piping system attached with PEA device mounted on the shaking table, and close-up view

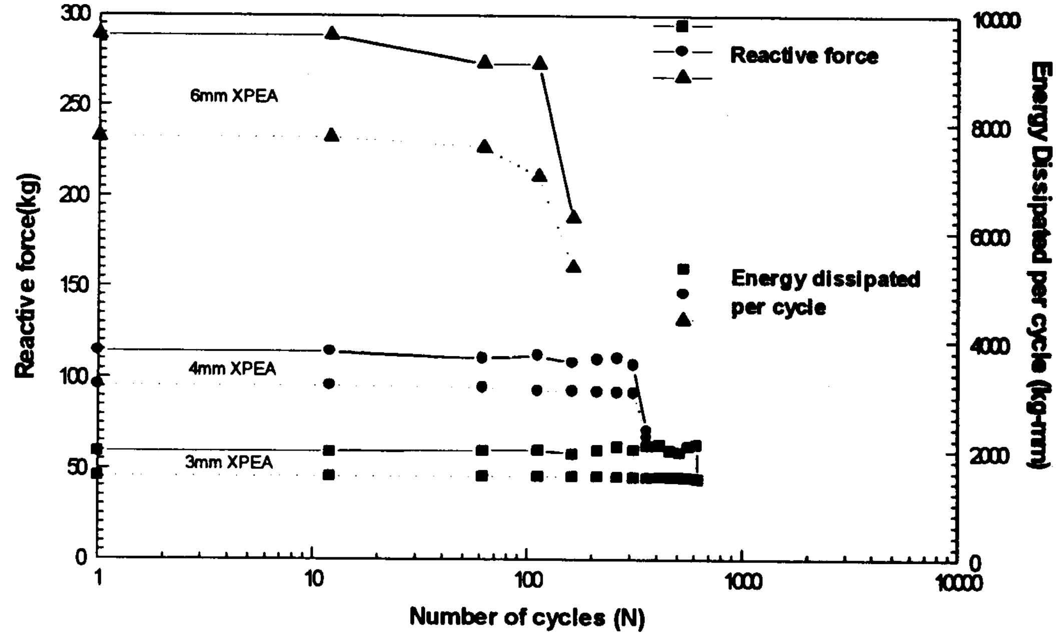

Fig. 5 Dynamic test results on different PEA elements at constant peak displacement amplitude of 15 mm at 3.0 Hz

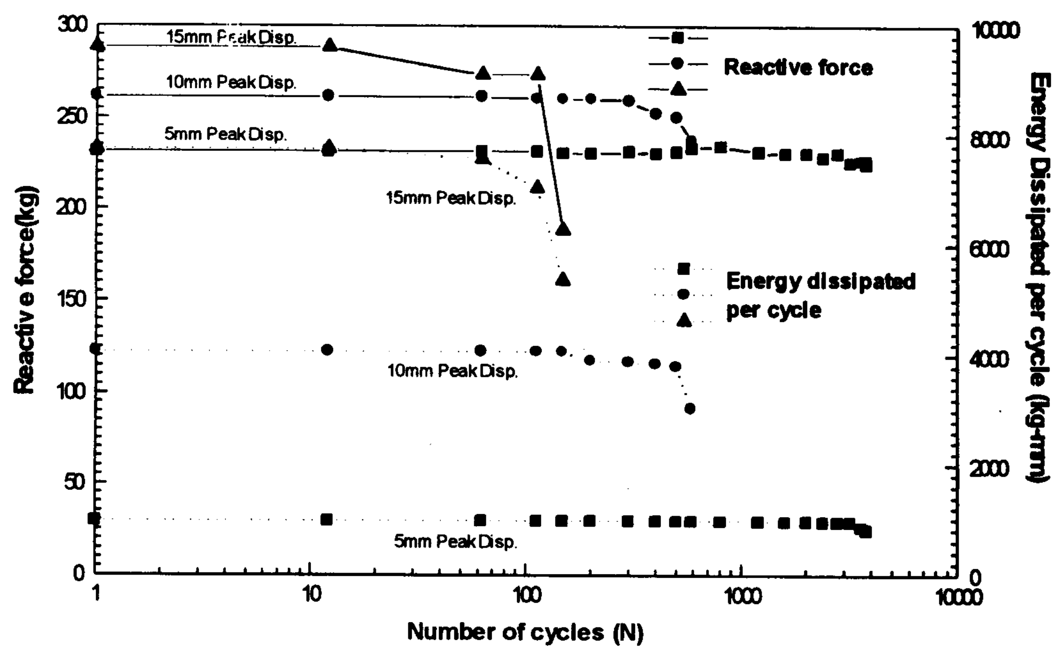

Fig. 6 Dynamic test results on 6 mm thick PEA elements at different displacement amplitudes at 3.0 Hz

5. Piping (3D) System

After having done the performance evaluation of PEA elements attached to a simple SDOF pipe element, the performance of the final PEA device made of independent PEA elements was studied from similar shaking table tests conducted on a complicated three-dimensional (3D) piping system, as shown in Figure 4. The piping system studied was made of three pipe segments, connected using elbow sections so that it spans in all three orthogonal directions, so that the resulting seismic response will be three-dimensional. However, the maximum seismic response of the 3D piping system was expected to occur in the direction of excitation. Evaluation of the seismic response for such

3D piping system using mathematical models is complicated, which makes shaking table tests mandatory. The 3D piping system studied was provided with suitable arrangements at the critical location for attaching the PEA device in the excitation direction, where maximum system response was expected to occur.

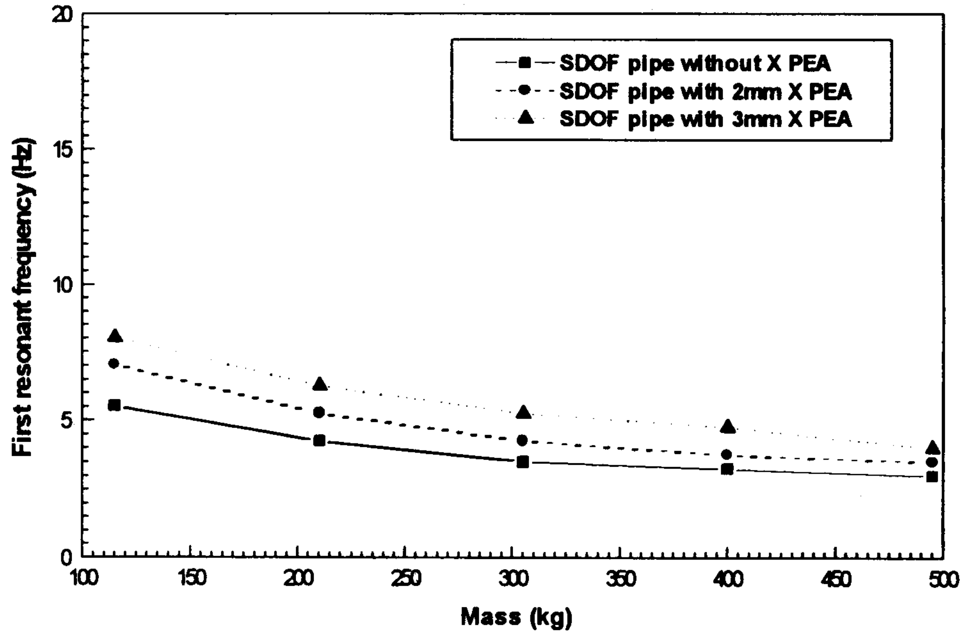

Fig. 7 Sweep sine test results on the SDOF pipe element attached with different PEA elements for different mass levels

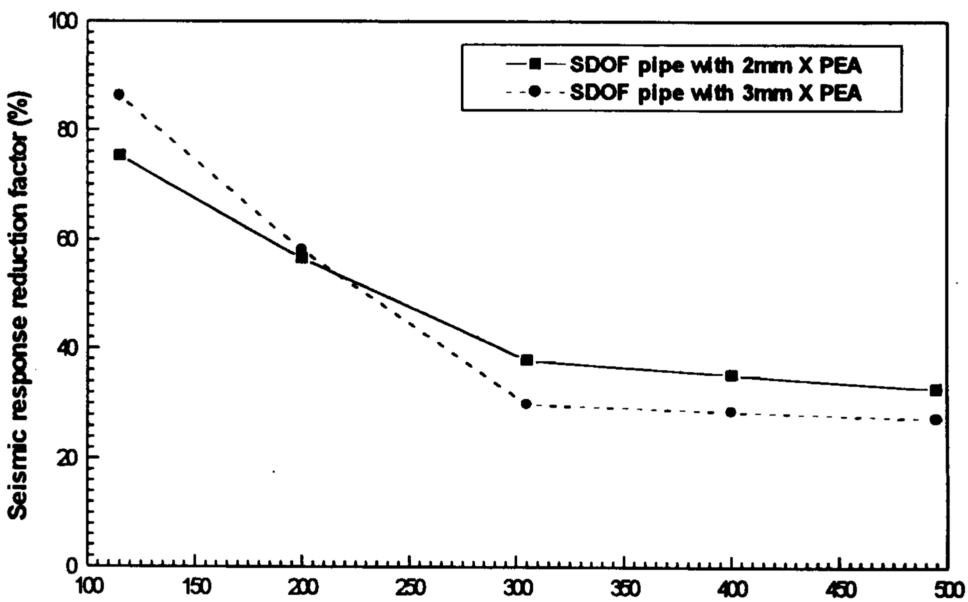

Fig. 8 Seismic test results on the SDOF pipe element attached with different PEA elements for different mass levels

6. Shaking Table Tests on the Piping (3D) System

Shaking table tests of sweep sine and seismic nature, as mentioned in the earlier section, were conducted on the 3D piping system initially, without the PEA device attached to it. The system dynamic characteristics like stiffness and damping were evaluated from the sweep sine test, and the seismic response was evaluated from the seismic test. Such tests were then repeated on the same piping system, with PEA device attached at the critical location, to study the seismic response reduction of the whole system. The combination of the PEA elements to be used for making the final PEA device was arrived at, based on the test results conducted on the SDOF pipe segment. By conducting the whole exercise for different peak amplitudes of the selected response spectrum, the seismic response reduction efficiency of the PEA device at different base excitation levels was evaluated. From the shaking table test results obtained, the suitability of such yielding type elasto-plastic PEA device, for supporting piping systems subjected to earthquake loading, was studied.

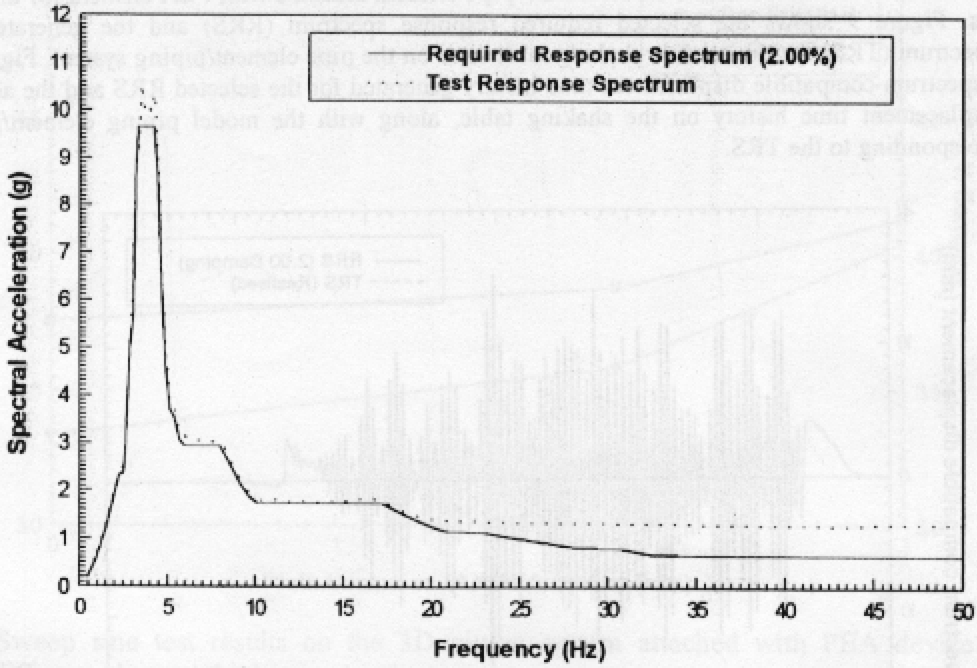

Fig. 9 Required response spectrum (RRS), and the generated test response spectrum (TRS) adopted for the shaking table tests on the SDOF pipe element and 3D piping system

TEST RESULTS AND OBSERVATIONS

Figure 5 shows the dynamic/fatigue test results conducted on different PEA elements at constant peak displacement amplitude of 15 mm at 3.0 Hz. From the reactive forces and force-displacement (hysteresis) curves obtained, the values of design stiffness and damping for the individual PEA were evaluated. The reactive force and the energy dissipated per cycle obtained from the dynamic tests of constant displacement amplitude showed an increasing trend with the increase in element thickness. PEA elements with 3 and 4 mm thickness showed stable hysteresis curves throughout the tests up to failure. This phenomenon of stable hysteresis curves throughout the design life is an important parameter in designing a PEA device for seismic response reduction. However, PEA element of 6 mm thickness did not show such a trend and showed a steep fall in the reactive force for the last few cycles. The failure was also observed to be a brittle failure. This is mainly due to the very large dynamic strains, induced in the element, resulting from very high reactive force realised due to the higher input displacement of 15 mm which is about 15 times the yield displacement. In order to improve the performance of such 6 mm thick PEA element, further dynamic tests of similar type were conducted on similar elements for different peak displacement values. This effort resulted in identifying the limiting value of design dynamic displacement, that can be applied to the element, up to which stable hysteresis curves are achieved. Figure 6 shows the dynamic/fatigue test results conducted on 6 mm thick PEA elements at different peak displacement amplitudes at 3.0 Hz. Based on these results, the design lives of different PEA elements were arrived at.

The basic requirement in adding a PEA element to the SDOF pipe system is to achieve more seismic response reduction, only by way of providing more supplemental damping to the system without altering its first resonant frequency. However, the addition of such PEA element to the SDOF pipe system will definitely result in an increase in the first resonant frequency. But the designer has to keep in mind that the change in the first resonant frequency can only be marginal for earthquake type loading. For the SDOF pipe system studied, the addition of PEA elements are found be more effective at higher mass levels above 300 kg. This was evident from the sweep sine tests results obtained on the SDOF pipe system. Below this mass level, the seismic response reduction is more due to the increased stiffness than to the supplemental damping from the PEA element added to the system. Figure 7 shows the sweep sine test results on the SDOF pipe element attached with/without PEA element for different mass levels. Figure 8 shows the seismic test results on the SDOF pipe element attached with PEA element for different mass levels. Figure 9 shows the selected required response spectrum (RRS) and the generated test response spectrum (TRS) for the seismic shaking table tests on the pipe element/piping system. Figure 10 shows the spectrum-compatible displacement time history generated for the selected RRS and the actually realised displacement time history on the shaking table, along with the model piping element/piping system, corresponding to the TRS.

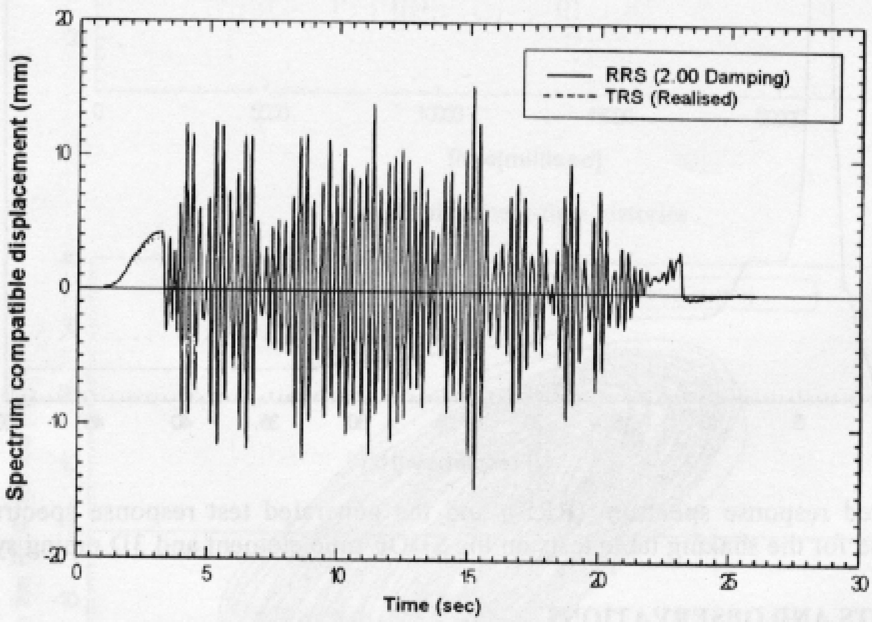

Fig.10 Spectrum compatible displacement time history for the selected RRS and the realised displacement time history corresponding to the TRS on the shaking table

From the low-amplitude sweep sine tests conducted on the 3D piping system, it was observed that both first resonant frequency and critical damping ratio were found to marginally increase due to the addition of PEA devices. Figure 11 shows the sweep sine test results on the 3D piping system attached with/without PEA device having X-plate element of two different thickness values. From the large amplitude seismic tests conducted on the 3D piping system attached with PEA device for different base excitation levels, say 10, 20, 30 & 40%, it was observed that the seismic response reduction factor of the system was found to decrease with the increase in the applied base excitation level. It was also observed that the seismic response reduction efficiency of 3 mm PEA device was found to be higher at all base excitation levels for the 3D piping system studied. Figure 12 shows the seismic test results on the same 3D piping system, attached with PEA devices, for different base excitation levels, thus showing the seismic response reduction efficiency of such devices under earthquake loading. Figure 13a shows typical seismic responses collected on the 3D piping system attached with/without PEA device, when subjected to seismic loading (40% base excitation level) on the shaking table. It was observed from the seismic tests that the attachment of PEA device to the 3D piping system is found to have two effects. One is the increase in the first natural frequency and the other is the addition in the system damping due to supplemental damping provided by the PEA device. It was also observed that the effect due to the increased stiffness is more at low base excitation levels (up to 20%) and marginal at high base excitation levels (above 20%). However, at higher base excitation levels (above 20%), the supplemental damping provided by the PEA device is found to have more effect in providing seismic response reduction to the

3D piping system. This was evident from the very low phase difference found in the seismic responses obtained on the 3D piping system before and after attaching the PEA device (vide Figure 13a). Similarly, Figure 13b shows the force-displacement hysteresis loops obtained in the PEA device attached to the 3D piping system, when subjected to seismic loading (40% base excitation level) on the shaking table. The large force-displacement hysteresis loops obtained under seismic loading from the PEA device show the role of energy dissipation added to the 3D piping system in reducing the seismic response.

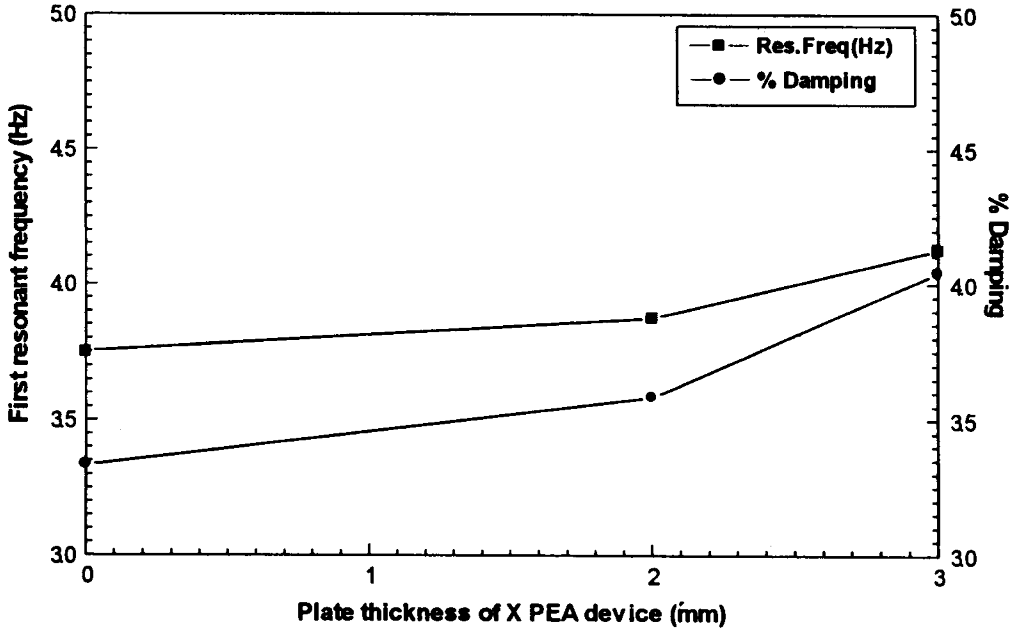

Fig.11 Sweep sine test results on the 3D piping system attached with PEA device having different element thickness

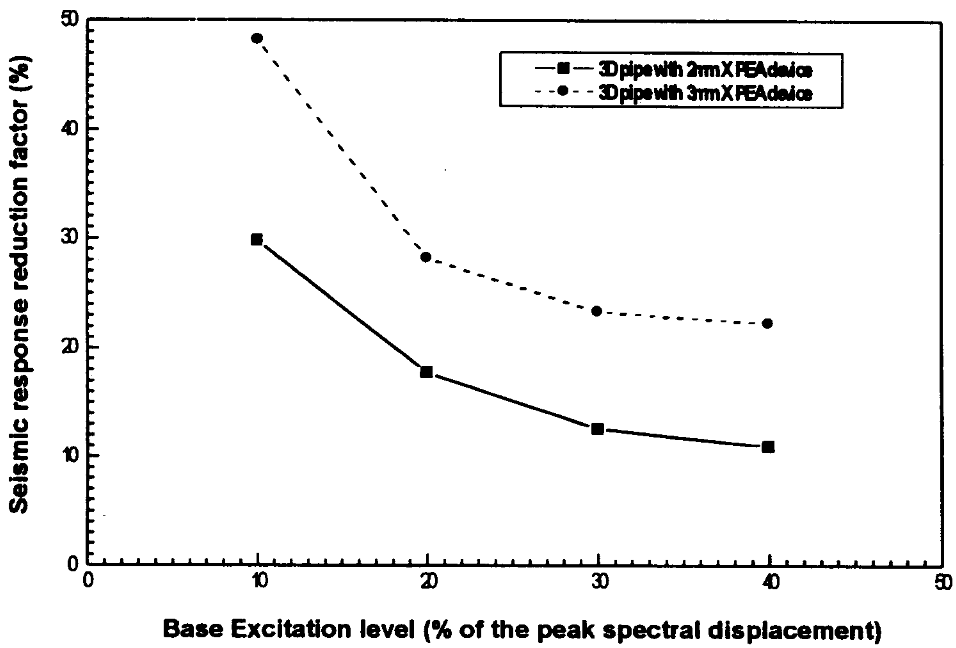

Fig.12 Seismic test results on the 3D piping system attached with PEA device having different element thickness for different base excitation levels

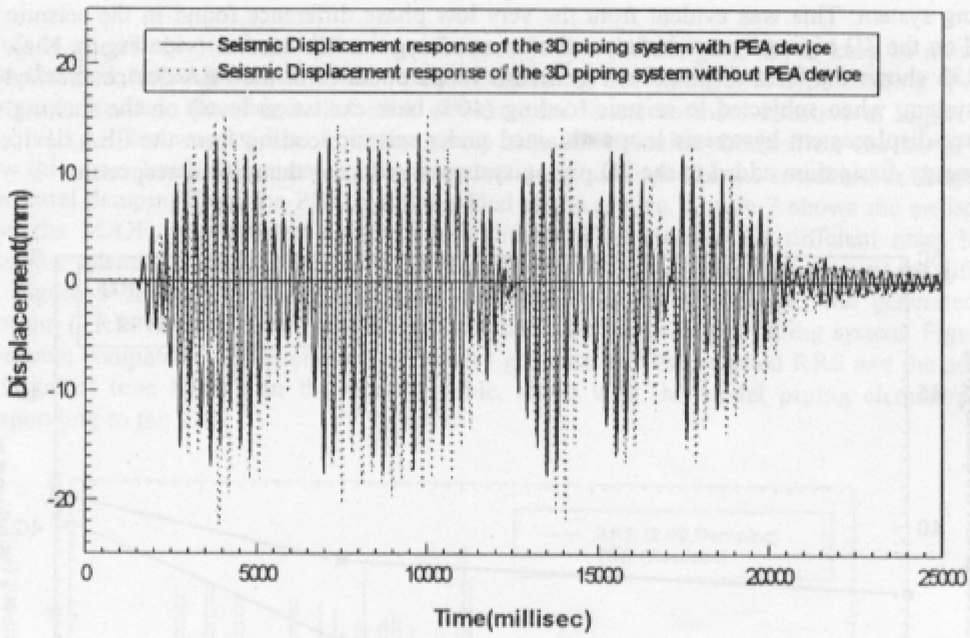

(a) Displacement-time histories

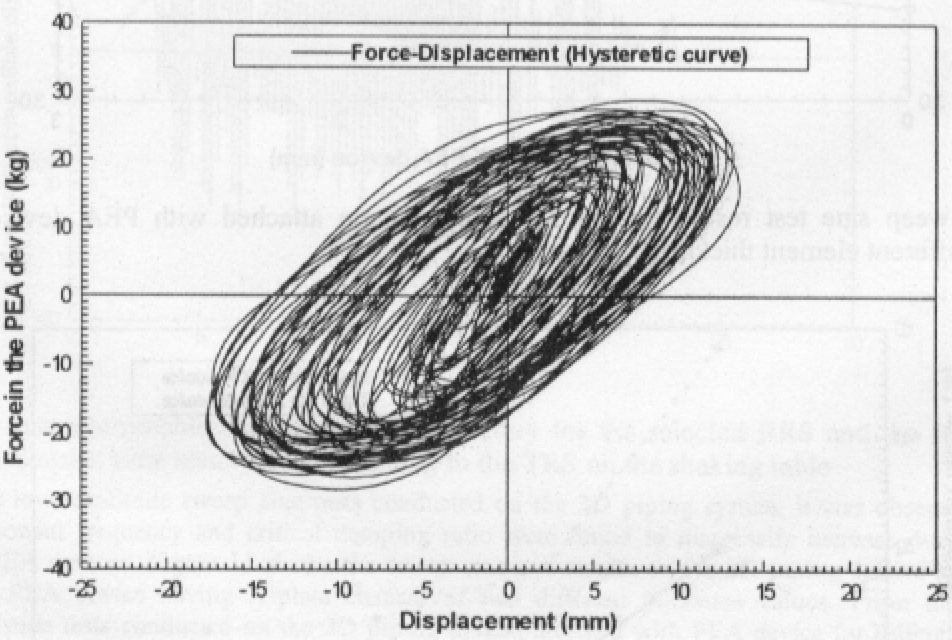

(b) Force-displacement curve

Fig.13 Typical seismic responses measured on the 3D piping system under earthquake loading

ANALYTICAL STUDY

1. Static Loading

The material characteristics of the X-shaped plate (vide Figure 14a), the elastic modulus (E), and the stress hardening rate (H), are expressed by the bi-linear model. The skeleton force-displacement curve (vide Figure 14b) of the X-shaped plate for each stress level was investigated using beam theory.

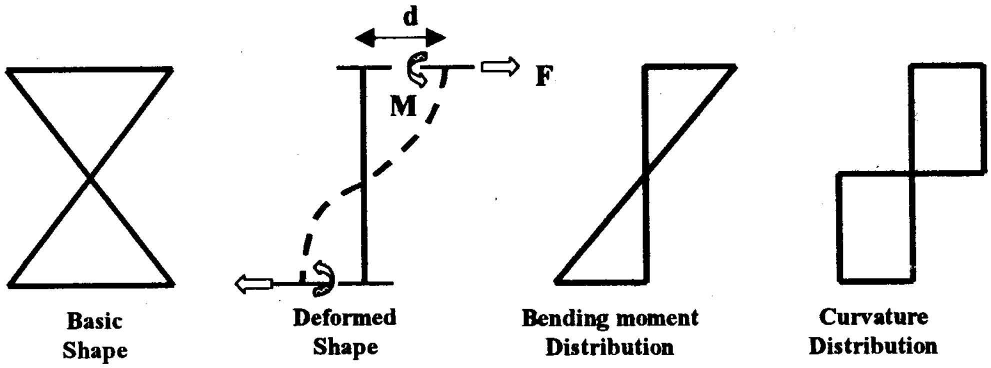

(a) X-plate PEA element

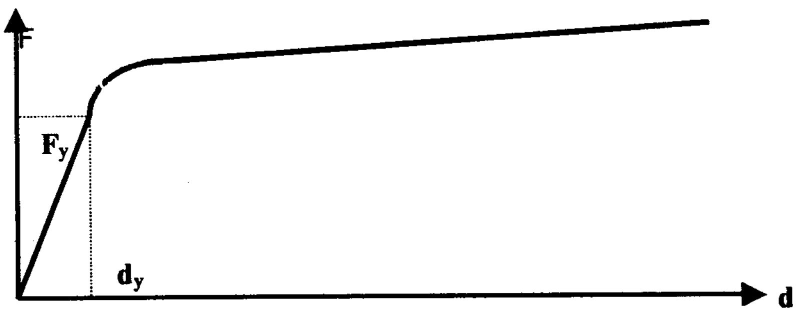

(b) Static force-displacement curve

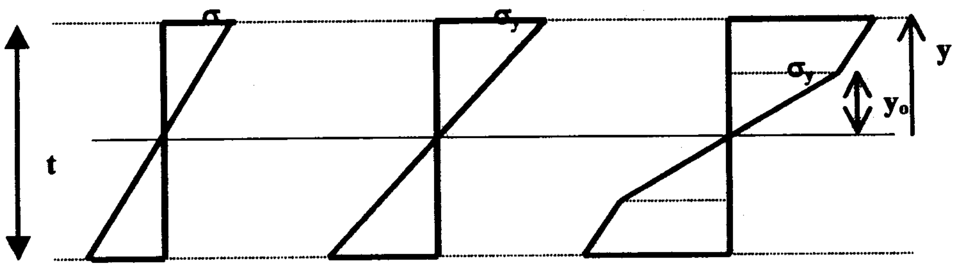

(c) Variation of stress across thickness at various stages of loading

Fig. 14 Analytical modeling of X-plate PEA element under static loading

In the elastic domain, the relation between the force (F) and the displacement (d) is given as follows:

$$F = \frac{Ebt^3n}{12a^3}d \quad \text{and the equivalent stiffness } K = \frac{Ebt^3n}{12a^3} \tag{1}$$

where, a is the height of the triangular plate, b is the maximum breadth, t is the plate thickness, and n is the number of X-plate PEA elements.

In the plastic domain (vide Figure 14c) at the yield point, the X-shaped plate surface is plastic and the plate surface stress is σ_y. Then the yield force (F_y) and the corresponding yield displacement (d_y) are given as follows:

$$F_y = \frac{\sigma_y t^2}{6}\frac{b}{a}n; \qquad d_y = \frac{2\sigma_y a^2}{Et} \tag{2}$$

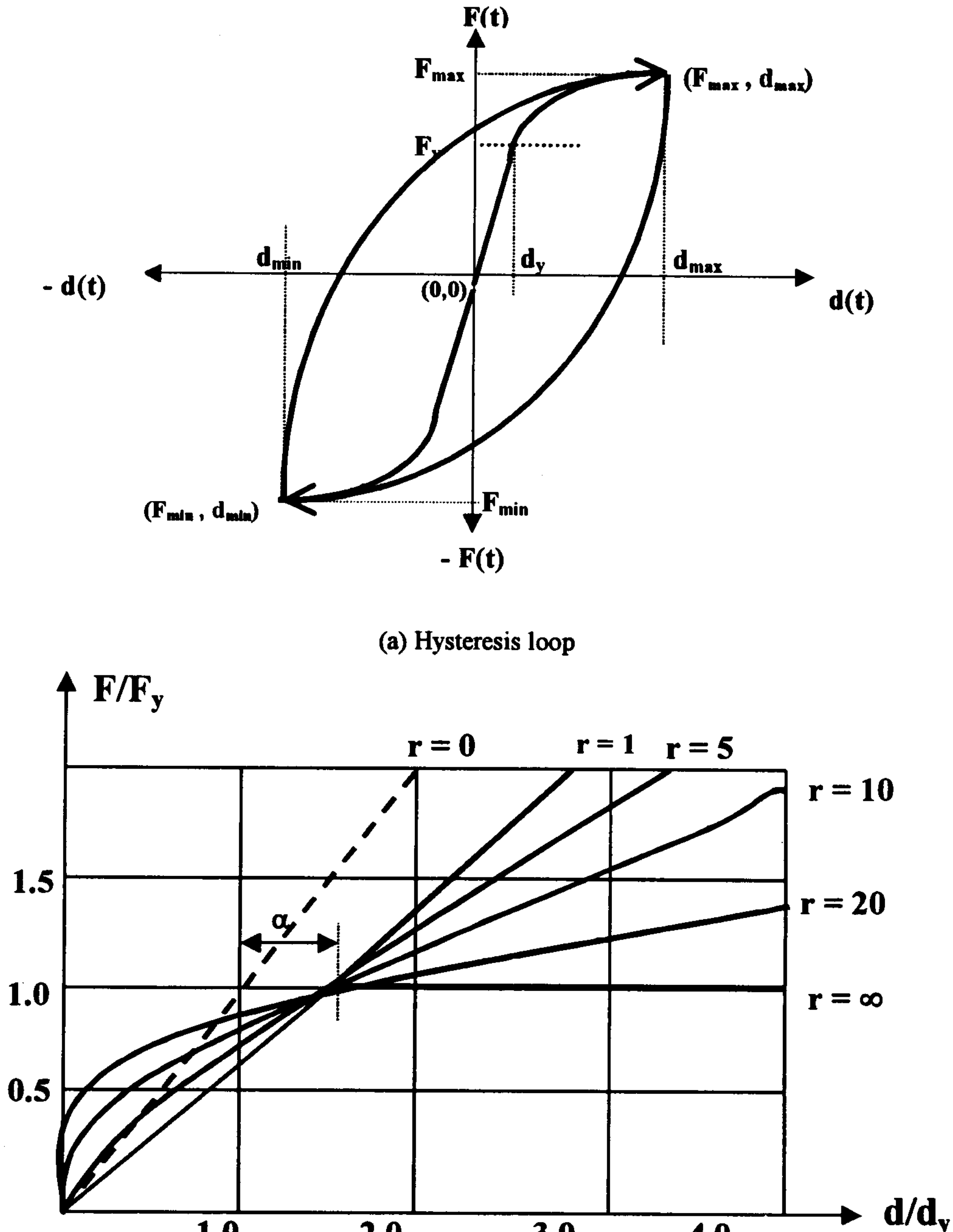

(a) Hysteresis loop

(b) Ramberg-Osgood function

Fig. 15 Ramberg-Osgood model adopted for modeling X-plate PEA under dynamic loading

Similarly, in the plastic region, considering the effect due to strain hardening rate (H), the force-displacement relation is given as follows:

$$F = \frac{nb\sigma_y}{12Ea}\left\{\left(4y_o^2 - 3t^2\right)\left(H - E\right) + H\frac{t^3}{y_o}\right\} \tag{3}$$

where, y_0 is the elastic depth, which can be evaluated using

$$y_o = \frac{\sigma_y a^2}{Ed} \tag{4}$$

The hysteresis loop can be obtained by giving the strain-stress characteristics of the very small part as bi-linear in each stress condition. The equivalent stiffness (K) and the element damping ratio (h) can show the dynamic characteristics of the PEA element. The former is obtained from the tangential stiffness at the reversal point of the skeleton curve. The latter is obtained as the ratio between the element strain energy and the dissipating energy per cycle (ΔE),

$$\Delta E = 3F_y(d + d_1) + \frac{d_y^{\,2} F_y}{(d + d_1)} - (3d_y F_y) - \left[Ft^2 / K\right] \tag{5}$$

$$h = \frac{\Delta E}{2\pi K d^2} \tag{6}$$

2. Dynamic/Cyclic Loading

In the elasto-plastic analysis of X-plate PEA elements under dynamic or cyclic loading, standard hysteretic models (Kelly et al., 1972; Sathish Kumar et al., 2000) are usually used, such as ideal elasto-plastic, bilinear, Bauschinger, Ramberg–Osgood, Takeda, Wen, and polygonal model. The basic form of the force-displacement model is selected, usually based upon an analogy with the plasticity theory, and then the model parameters are determined via a curve-fitting procedure.

Of all the hysteretic models stated, the Ramberg–Osgood model (Kelly et al., 1972; Sathish Kumar et al., 2000) developed by Jennings suits closely to such X-shaped PEA elements, and hence is adopted in the experimental study at the element level, to evaluate the equivalent stiffness and damping of X-shaped PEA elements required for designing the PEA device. However, the Ramberg-Osgood model chosen does not consider the stiffness degradation in successive cycles for such X-shaped PEA elements, subjected to cyclic loading, resulting in ever-increasing hysteresis loops. The Ramberg-Osgood model essentially establishes a power-law relationship between the force and inelastic displacement, and consequently, is effective in modeling the response of a variety of metals under cyclic/dynamic loading. This model approximates the shape of the force-displacement curve $[F(t)$ versus $d(t)]$ by appropriate selection of the auxiliary parameters (vide Figure 15) called Ramberg-Osgood exponent (r) and Jennings constant (α), according to the shape of the actual hysteretic curve. In the present study, the values of these auxiliary parameters were realistically evaluated from the static test results by using curve-fitting procedure. The force-displacement relations at various stages in the hysteresis loop were obtained by using the following expressions:

(i) for the basic loading branch of the hysteresis loop between the coordinates (0,0) and (F_{max}, d_{max}),

$$\frac{d(t)}{d_y} = \frac{F(t)}{F_y}\left(1 + \alpha\left(\text{abs}\left(\frac{F(t)}{F_y}\right)\right)^{r-1}\right) \tag{7}$$

(ii) for the unloading branch of the hysteresis loop between the coordinates (F_{max}, d_{max}) and (F_{min}, d_{min}),

$$\frac{d(t) - d_{max}}{d_y} = \frac{F(t) - F_{max}}{F_y}\left(1 + \alpha\left(\text{abs}\left(\frac{F(t) - F_{max}}{2F_y}\right)\right)^{r-1}\right) \tag{8}$$

(iii) for the reloading branch of the hysteresis loop between the coordinates (F_{min}, d_{min}) and (F_{max}, d_{max})

$$\frac{d(t) - d_{min}}{d_y} = \frac{F(t) - F_{min}}{F_y}\left(1 + \alpha\left(\text{abs}\left(\frac{F(t) - F_{min}}{2F_y}\right)\right)^{r-1}\right) \tag{9}$$

The hysteretic energy dissipation index (h) of the X-plate PEA element using the Ramberg-Osgood model is expressed as follows:

$$h=\frac{2}{\pi}\left(1-\frac{2\alpha}{r+1}\right)\left(1-\frac{d_y F_{max}}{F_y d_{max}}\right) \tag{10}$$

Figure 16 shows the comparison between the theoretical and experimental results under static loading on a 4 mm thick X-plate PEA element. Similarly, Figure 17 shows the comparison between the theoretical and experimental results under dynamic loading on a 4 mm thick X-plate PEA element at 3.0 Hz with maximum peak displacement amplitude of 15 mm. The type of dynamic loading adopted was a sinusoidal constant displacement loading, initially enveloped with a linearly ramping-up function for the first 10 cycles.

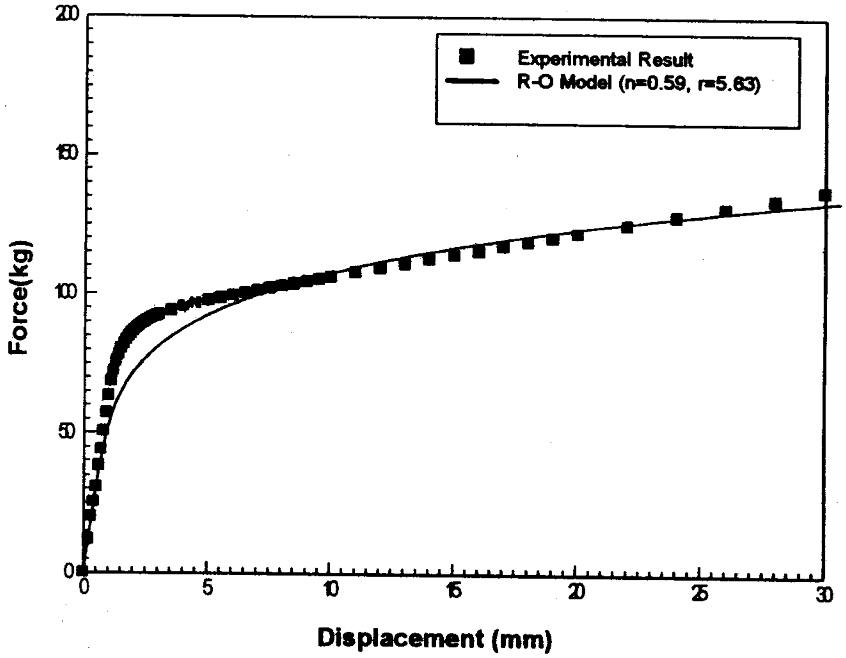

Fig.16 Comparison between theoretical and experimental results under static loading on a 4 mm thick X-plate PEA element

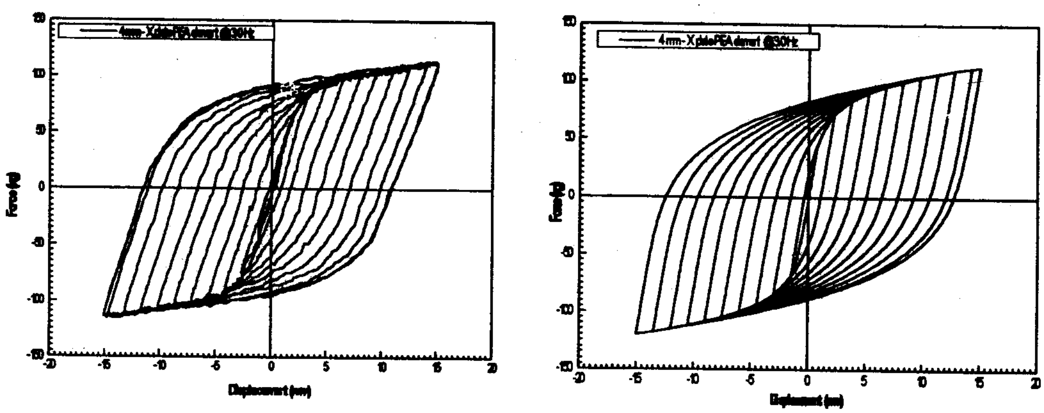

(a) Experimental curve (b) Theoretical curve

Fig.17 Comparison between theoretical and experimental results under dynamic loading at 3.0 Hz on a 4 mm thick X-plate PEA element

SUMMARY AND CONCLUSIONS

Static and dynamic tests were conducted on yielding type X-plate PEA elements of three different thicknesses, to study their suitability for designing an elasto-plastic PEA device for supporting complicated piping systems subjected to seismic loading. Test results showed that the PEA elements studied were effective in providing energy dissipation to the system in the form of large hysteresis loops. Stable hysteresis loops were observed under dynamic loading up to failure, showing the ability of these elements in providing uniform energy dissipation throughout their design life. Based on the end results, the safe design lives for different yielding type X-plate PEA elements were arrived at. Ramberg-Osgood (RO) model was used to predict the force-displacement characteristics of the X-plate PEA element subjected to static and dynamic loading. The auxiliary parameters r and α required for modeling were evaluated from the static test results by using a standard curve-fitting procedure. Using the developed RO model, the force-displacement responses of different X-plate PEA elements under static/dynamic loading were theoretically evaluated and compared against the experimentally measured responses. From the close match found between the analytical and experimental responses, obtained on different X-plate PEA elements under static/dynamic loading, the Ramberg-Osgood model for evaluating the design parameters of the individual PEA element, required for designing PEA devices, was validated.

Shaking table tests of sweep sine and seismic nature were conducted on a SDOF pipe before and after attaching PEA element of two different plate thicknesses. The response reduction efficiency of the PEA element under seismic loading was evaluated from the responses collected on the SDOF pipe before and after attaching the PEA element at the free end. The effect due to mass level at the free end, on the seismic response reduction efficiency of different PEA elements, was also studied. The end results showed that the addition of such a PEA element is more effective only at higher mass levels, in providing supplemental damping to the SDOF pipe for reduced seismic response. However, at lower mass levels, increased stiffness due to the addition of PEA element is found to dominate in providing seismic response reduction to the SDOF pipe studied. Based on the end results, a yielding type elasto-plastic PEA device made of X-plate PEA elements was developed.

Similar shaking table tests of sweep sine and seismic nature were conducted on a 3D piping system, before and after attaching PEA device having two different plate thicknesses. The response reduction efficiency of the PEA device under seismic loading was evaluated from the responses collected on the 3D piping system, before and after attaching the PEA device at the critical location in the excitation direction. The effect due to the base excitation level on the seismic response reduction efficiency of different PEA devices was also studied. The end results showed that the yielding type elasto-plastic PEA device made of X-plate PEA elements was effective in reducing the system seismic response by way of providing supplemental damping. However, the seismic response reduction efficiency tends to decrease with the increase in the base excitation level. These observations prove the efficiency of yielding type PEA devices, made using X-shaped metal plate elements, in reducing the response of complicated piping systems to any unforeseen event like earthquake.

ACKNOWLEDGEMENTS

The authors wish to express their deep appreciation to Director, SERC, Chennai and Head, Reactor Safety Division, Bhabha Atomic Research Centre, Mumbai, for their valuable advice and kind permission to publish the combined research work carried out.

REFERENCES

1. Chiba, Y. and Kobayashi, H. (1992). "Response Characteristics of Piping System Supported by Visco-Elastic and Elasto-Plastic Dampers", Transactions of the ASME on Pressure Vessel Technology, Vol. 112, pp. 34-38.
2. Gopalakrishnan, N., Sathish Kumar, K., Muthumani, K. and Sivarama Sarma, B. (2001). "Evaluation of Seismic Response of a Pipe Element with X-Type Metal Passive Energy Absorbers", Technical Report, SERC, Chennai.

3. Kelly, J.M., Skinner, R.I. and Heine, A.J. (1972). "Mechanism of Energy Absorption in Special Devices for Use in Earthquake Resistant Structures", Bull. New Zealand Soc. Earthquake Engineering, Vol. 5, No. 3, pp. 63-88.

4. Kokubo, E., Fujita, K., Fuyama, H. and Ichihashi, I. (1995). "Development of a Lead Extrusion Damper for PWR Reactor Coolant Loop System", ASME Special Publication on Seismic Engineering, PVP-Vol. 312, pp. 425-431.

5. Namita, Y., Shigeta, M., Yoshinaga, T., Gotoh, N. and Kawahata, J. (1991). "The Application of Elastoplastic Support Devices for a Piping System", Proceedings of JSME International Journal, Series III, Vol. 34, No. 1, pp. 42-47.

6. Sathish Kumar, K., Muthumani, K., Sivarama Sarma, B. and Gopalakrishnan, N. (2000). "Evaluation of X-Type Metal Passive Energy Absorbers", Technical Report, SERC, Chennai.

7. Sivarama Sarma, B., Sathish Kumar, K., Gopalakrishnan, N. and Muthumani, K. (2001). "Evaluation of Seismic Response of a 3-D Pipe System with X-Type Metal Passive Energy Absorbers", Technical Report, SERC, Chennai.

8. Skinner, R.I., Kelly, J.M. and Heine, A.J. (1975). "Hysteresis Dampers for Earthquake Resistant Structures", Earthquake Engineering and Structural Dynamics, Vol. 3, pp. 287-296.